energies

Article

Hybrid Optimization-Based Sequential Placement of DES in Unbalanced Active Distribution Networks Considering Multi-Scenario Operation

Ruihua Si [1], Xintong Yan [1], Wanxun Liu [1], Ping Zhang [1], Mengdi Wang [2], Fengyong Li [2], Jiajia Yang [3,*] and Xiangjing Su [2,*]

[1] State Grid Henan Economic Research Institute, Zhengzhou 450052, China
[2] Offshore Wind Power Research Institute, Shanghai University of Electric Power, Shanghai 200090, China
[3] College of Science and Engineering, James Cook University, Townsville 4811, Australia
* Correspondence: jiajia.yang@jcu.edu.au (J.Y.); xiangjing.su@shiep.edu.cn (X.S.); Tel.: +61-4-03590976 (J.Y.); +86-13601846568 (X.S.)

Abstract: The increasing penetration of distributed generation (DG) brings about great economic and environmental benefits, while also negatively affecting the operation of distribution networks due to its high intermittency. Although distributed energy storage (DES) can effectively deal with the problems caused by massive DG penetrations by decoupling the generation and consumption of electricity, the placement of DES significantly determines the effectiveness of its capabilities. Unfortunately, existing DES placement studies are commonly based on a balanced network model, whereas practical distribution networks are unbalanced. In addition, existing DES placement studies are mostly based on an extreme scenario and rarely consider the operational complexity resulting from the uncertainties of DGs and loads. To address the aforementioned challenges, this paper proposes a hierarchical and sequential DES placement strategy in distribution networks by considering multi-scenario operations. Specifically, the proposed hierarchical framework for DES placement includes three sequential layers: outer, inter, and inner. In the outer layer, a multi-scenario comprehensive loss sensitivity index (MSCLSI) is first introduced to search for the most effective DES placement location. Subsequently, the sizing and scheduling of DES for the selected location are conducted through coordinated optimization across the inter and inner layers, which can be solved using a hybrid method combining particle swarm optimization and second-order cone programming (PSO-SOCP). Finally, a series of detailed simulations are carried out over the IEEE-33 test system and the experimental results demonstrate that the proposed scheme can provide significant effectiveness and superiority compared to the state-of-the-art schemes.

Keywords: distributed energy storage; optimal placement; hybrid optimization

Academic Editors: Frede Blaabjerg and Xiaohuan Zhao

Received: 12 November 2024
Revised: 13 January 2025
Accepted: 16 January 2025
Published: 21 January 2025

Citation: Si, R.; Yan, X.; Liu, W.; Zhang, P.; Wang, M.; Li, F.; Yang, J.; Su, X. Hybrid Optimization-Based Sequential Placement of DES in Unbalanced Active Distribution Networks Considering Multi-Scenario Operation. *Energies* **2025**, *18*, 474. https://doi.org/10.3390/en18030474

1. Introduction

To address sustainability and environmental issues, distributed generations (DGs) have been developing rapidly worldwide [1]. Meanwhile, the growing integration of DG may negatively impact the operation of distribution networks because, due to its high intermittency and uncertainty, operation issues arise, such as reverse power flow, frequent voltage violation and serious power loss [2]. The mismatch between load and DG also causes a larger peak–valley difference and a higher energy cost [3]. For the issues mentioned above, distributed energy storage (DES) provides the most effective solutions by decoupling generation and consumption times and storing lower-cost off-peak energy while discharging it during peak hours [4–6]. However, due to the still high price, the DES potential benefits are highly related to its optimal placement [7].

Generally, DES placement involves the selection of battery type, installation location, energy capacity and the charging/discharging power schedule [8]. By far, the problem of DES placement has been widely studied. For example, in [9], the study aimed to determine the optimal placement and capacity of the DES in the IEEE 33- and 69-bus distribution systems connected with PV and EV penetrations by considering overall system costs, which include investment, replacement, operation and maintenance costs as the objective functions to be minimized. In [10], given installation locations, a DES placement model considering conservation voltage reduction was proposed to determine the optimal DES size for reduced investment and operation costs. In [11], the DES placement was formulated as a duck curve phenomenon and optimized using a metaheuristic algorithm with high exploration and exploitation ability, known as the Whale Optimization Algorithm (WOA). Considering the budget limit, the optimal placement of DES in power networks was formulated in [12] for load shifting and generation cost reduction. In [13], a newly proposed optimization algorithm named the crayfish optimization algorithm (COA) was applied to solve the problem of DES placement. A heuristic optimization strategy based on voltage sensitivity analysis was used in [14] to determine the optimal placement (number, locations, sizes) of ESSs and prevent voltage violations.

Nevertheless, as power systems grow in scale and precision, the computation challenge of any optimization approach to solving an OPF DES placement problem increases exponentially [15]. To minimize the computation and memory demands of DES placement in complex distribution networks, a common practice is to conduct a sensitivity analysis and pre-select the locations with the highest sensitivities [16]. The power injection (i.e., discharging) model is used in current sensitivity calculations for DES placements, although DES uses bidirectional flow, which has opposite impacts on sensitivity. To address the above-mentioned challenges on sensitivity and unbalance, our previous study proposed a CLSI-based sequential DES placement strategy to allow more practically feasible and appropriate locations in distribution networks [17]. However, reference [17] only considered a CLSI based on a single operation scenario, which makes the results difficult to apply to the actual operation situation. Also, the optimization algorithm (PSO) used in reference [17] caused the computation process to be time-consuming and complicated, infeasible for the large-scale unbalanced distribution networks of this study.

Although previous studies have made certain progress, three technical issues have not been well addressed so far. Firstly, the previous studies were usually based on a fixed extreme operation scenario, while the uncertainties of DGs and load may cause the operation of distribution networks to be more complicated. Thus, a single fixed scenario cannot represent real operations well, causing the DES placement solutions to be less effective. Secondly, the previous sensitivity methods were always based on a single fixed scenario, making it difficult to cope with complex operational scenarios, especially in large-scale DG-integrated distribution networks. Thirdly, DES placement can be solved through heuristic searches or mathematical programming methods, but due to a series of assumptions and approximations, it is easy to produce suboptimal or even infeasible solutions. Meanwhile, the global optimal solution of heuristic searches can also easily lead to high time consumption.

To address the challenges above, this study proposes a hybrid optimization-based sequential placement model for the optimal siting, sizing and scheduling of DESs in distribution networks. The main contributions of this paper are as follows.

- A multi-scenario comprehensive loss sensitivity index (MSCLSI) is redefined, which determines the DES installation location by considering the impacts of both DES charging and discharging under typical seasonal operation scenarios.
- A sequential DES placement strategy is proposed to decide the siting of all DESs in distribution networks sequentially. For each placement, the optimal sizing and operation scheduling of DES under multiple operation scenarios is formulated for the maximum economic benefits.
- A hybrid solution strategy of PSO and SOCP is further proposed to balance the solution optimality and computation efficiency, making the proposed placement model suitable for large-scale unbalanced distribution networks.

The rest of this paper is organized as follows. Section 2 reviews the integrated DES sizing and scheduling model. Furthermore, we provide a detailed explanation of the proposed hybrid solution in Section 3 and present a MSCLSI-based sequential placement strategy in Section 4. Subsequently, we implement a series of case studies to evaluate the performance of our scheme and show the corresponding experimental discussions in Section 5. Finally, Section 6 concludes the paper.

2. Integrated DES Sizing and Scheduling Model

2.1. Storage Type Selection

Existing energy storage types can be mainly categorized into electrical, mechanical, electrochemical and thermal energy storage according to the form of energy storage. Among them, electrochemical energy storage has been becoming an international research focus, due to its advantages in terms of site requirement, response time, conversion efficiency and size expandability. In this study, the DES placement is proposed for unbalanced active distribution networks with high renewable penetrations to enhance the network operation safety and economic benefits within the planning cycle. Thus, as the most advanced and developed electrochemical energy storage, lithium-ion battery storage is selected for its higher power, larger capacity, longer life cycle and lower maintenance requirements. It should be noted that the energy storage placement model proposed in this study is generic and can be adjusted for other types of energy storage.

2.2. DES Placement Objective Function

An integrated DES sizing and scheduling model is proposed here to minimize costs and maximize savings. Specifically, the objective function is defined to reduce the cost of DES investment CI, the cost of DES maintenance CM, and the cost of DES degradation CD, while increasing the savings through DES auxiliary services of load shifting SLS and loss reduction SLR.

$$Min\ OF = CI + CM + CD - SLR - SLS \tag{1}$$

(1) Cost of DES investment:

The cost of purchasing DES is included as the equivalent annual cost of the original investment and relevant fixed investments of DES installation:

$$CI = \sum_{p=1}^{3} \sum_{i \in N_{chosen}} \delta_B \cdot E_{B,i}^{p} \cdot \frac{r(1+r)^Y}{(1+r)^Y - 1}, \tag{2}$$

where δ_B and $E_{B,i}^{p}$ are the annual cost factor and energy capacity of DES at phase p, bus i, with $E_{B,i}^{p}$ calculated by

$$E_{B,i}^{p} = BN_i^p \times E_N, \tag{3}$$

where N_i^p is the number of batteries installed in phase p of node i; E_N is the rated capacity of individual batteries, Y is the DES useful life and r is the investment discount factor.

(2) Cost of DES maintenance:

The cost of DES maintenance refers to the expenses that need to be incurred during the operation of DES in order to ensure its normal operation, maintenance and management. The definition is as follows:

$$CM = \varepsilon_b \cdot \sum_{p=1}^{3} \sum_{i \in N_{chosen}} E_{B,i}^{p} \cdot \frac{r(1+r)^r}{(1+r)^Y - 1}, \tag{4}$$

where ε_b is the annual maintenance cost of DES, N_{chosen} configures a collection of nodes for DES, $E_{B,i}^p$ is the annual cost factor and energy capacity of DES at phase p, bus i, Y is the DES useful life and r is the investment discount factor.

(3) Cost of DES degradation:

During the placement cycle of DES, its life span will be reduced. Accordingly, the degradation cost of DES is considered and defined as follows:

$$CD = \sum_{t=1}^{T} \delta \cdot \left(\left| p_{i,t}^{p} \right| + \eta_L \cdot E_{B,i}^{p} \cdot \Delta t \right) \cdot \frac{r(1+r)^r}{(1+r)^Y - 1}, \tag{5}$$

where T is the typical daily scheduling cycle, δ is the cost factor for DES life loss, $p_{i,t}^p$ is the charging/discharging power of phase p at node i and η_L is the DES leakage factor.

(4) Savings of DES loss reduction:

The yearly savings from reducing energy loss are calculated by the sum of savings under multiple operation scenarios and different load levels, pre- and post-installation of the DES (represented as $P_{Loss,t}$ and $P'_{Loss,t}$).

$$SLR = \sum_{s=1}^{S} \sum_{l=1,3} \sum_{t=1}^{T} \left(P_{Loss,t} - P'_{Loss,t} \right) \cdot e_l \tag{6}$$

In Equation (6), $P_{Loss,t}$ is defined by

$$P_{Loss,t} = \sum_{\beta=1}^{N-1} \mathrm{Re} \left\{ \begin{bmatrix} I_{\beta,t}^{\alpha\,*} & I_{\beta,t}^{b\,*} & I_{\beta,t}^{c\,*} \end{bmatrix} \begin{bmatrix} Z_\beta^{aa} & Z_\beta^{ab} & Z_\beta^{ac} \\ Z_\beta^{ba} & Z_\beta^{bb} & Z_\beta^{bc} \\ Z_\beta^{ca} & Z_\beta^{cb} & Z_\beta^{cc} \end{bmatrix} \begin{bmatrix} I_{\beta,t}^{\alpha} \\ I_{\beta,t}^{b} \\ I_{\beta,t}^{c} \end{bmatrix} \right\}, \tag{7}$$

to consider the impacts of branch self (i.e., Z_β^{aa}, Z_β^{bb} and Z_β^{cc}) and mutual (i.e., Z_β^{ab}, Z_β^{bc}, Z_β^{ca}, etc.) phase coupling in unbalanced networks [18]. $I_{\beta,t}^p$ is the current through the phase p of branch β at time t.

(5) Savings of DES load shifting:

In existing studies, energy storage systems mainly participate in auxiliary services through frequency regulation and load peak regulation [19–21]. Considering the DES considered in this study is only used for distribution networks, and cannot support system frequency regulation, only the savings of load shifting are considered here and defined as an objective function. The market incentive from DES participation in the peak-shaving valley-filling auxiliary service is determined by the amount of electricity charged with the energy storage device during the peaking period and the corresponding compensation price, which is expressed as follows:

$$SLS = \sum_{t=1}^{T^v} p_{i,t}^{v} \cdot \Delta t \cdot \lambda_{sub}, \tag{8}$$

where T^v is the DES peaking period, $p^v_{i,t}$ is the scheduling when DES participates in peaking at t and λ_{sub} is the price of DES participation in peaking compensation.

The savings including SLR and SlS take into account optimization scenario variations and net load (i.e., load minus DG) profiles. Four typical season scenarios: spring, summer, autumn and winter (denoted, respectively, by $s = 1$, 2, 3 and 4) are used to represent different optimization scenarios where the network net load profile is categorized into three typical levels—high, medium and low—based on the load factor, represented by l = 1, 2 and 3, respectively [22].

2.3. DES Placement Constraints

The proposed integrated DES sizing and scheduling model should satisfy the constraints of unbalanced network operation, DES operation and decision variables.

(1) Power flow equations:

For distribution networks, power flow equations in the form of DistFlow are employed in this study, as given in Equations (9)–(11) [23].

$$P^p_{DG,i} + P^p_{ij} - \sum P^p_{jk} = -P^p_j + r^p_{ij}\frac{\left(P^p_{ij}\right)^2 + \left(Q^p_{ij}\right)^2}{\left(V^P_i\right)^2}, \tag{9}$$

$$Q^p_{DG,i} + Q^p_{ij} - \sum Q^p_{jk} = -Q^p_j + x^p_{ij}\frac{\left(P^p_{ij}\right)^2 + \left(Q^p_{ij}\right)^2}{\left(V^P_i\right)^2} \tag{10}$$

$$\left(V^P_i\right)^2 - \left(V^P_j\right)^2 = 2\left(r^p_{ij}P^p_{ij} + x^p_{ij}Q^p_{ij}\right) - \left(\left(r^p_{ij}\right)^2 + \left(x^p_{ij}\right)^2\right)\frac{\left(P^p_{ij}\right)^2 + \left(Q^p_{ij}\right)^2}{\left(V^P_i\right)^2} \tag{11}$$

Here, P^p_{ij}/Q^p_{ij} denote the active/reactive power through the branch between nodes i and j at phase p while r^p_{ij}/x^p_{ij} represent the branch resistance and reactance. $P^p_{DG,i}/Q^p_{DG,i}$ and P^p_j/Q^p_j represent the active/reactive DG outputs and load power at phase p buses i, j while V^P_i, V^P_j denote their voltage magnitudes. $\sum P^p_{jk}$ is the sum of the load active power transmitted through the branch between buses j and k at phase p, where k are nodes connected with node j except node i.

(2) Nodal voltage constraint:

The voltage magnitude of each node in the distribution networks should be within the boundary limits set by network operators at any time moment.

$$V_{min} < V^p_{i,t} < V_{max} \tag{12}$$

(3) Branch current constraint:

The current running through each branch should be lower than its current rating to reduce thermal loss.

$$I^p_{\beta,t} \le I_{max} \tag{13}$$

(4) DES operation constraint:

The enerDecision variables constraintgy charged and discharged during the operation period T should be equal, and the state of charge (SOC) should also within the boundary limits.

$$\sum\nolimits_{p=1}^{3} \sum\nolimits_{t=1}^{T} p^p_{i,t} = 0 \tag{14}$$

$$SOC^{min} \leq SOC_{i,1} + \frac{\sum_{p=1}^{3}\sum_{t=1}^{h} p_{i,t}^{p}\cdot 1}{\sum_{p=1}^{3} E_{B,i}^{p}} \leq SOC^{max} \tag{15}$$

(5) Decision variables constraint:

For the OPF problem of DES placement above, decision variables are the DES capacity and its daily scheduling under multiple operation scenarios. The decision variables are subject to constraints, with the maximum capacity (denoted by E_{Bmax}) typically determined by the project objectives and budget, while the maximum charging/discharging power is defined by its participation in the auxiliary services market and energy capacity.

$$0 \leq E_{B,i}^{p} \leq E_{Bmax} \tag{16}$$

$$-E_{B,i}^{p} \leq p_{i,t}^{p} \leq E_{B,i}^{p} \tag{17}$$

$$0 \leq p_{i,t}^{p} \leq f_1 \cdot P_{max}^{DES} \tag{18}$$

P_{max}^{DES} is the maximum charging and discharging power of DES; f_1 represents the sign variables of DES in the peaking auxiliary service market.

3. Hybrid Solution to the Proposed DES Placement OPF Problem

3.1. Decomposition of the Proposed DES Placement OPF Problem

The integrated DES sizing and scheduling problem in Equations (1)–(18) is essentially a mixed integer nonlinear programming (MINLP) problem with both discrete (i.e., energy capacity) and continuous (i.e., charging/discharging power) variables. Existing heuristic search or mathematical programming methods make it hard to balance the efficiency and accuracy of solutions. Thus, a hybrid solution strategy combining heuristic searches and mathematical programming is proposed considering the OPF problem. Hybrid optimizations can achieve significant improvements over each individual [24].

Specifically, the proposed OPF problem consists of two parts, i.e., DES sizing and scheduling under multiple scenarios, which is a mixed integer nonlinear programming problem with discrete sizing variables. Separate heuristic algorithms or mathematical planning methods are unable to solve the OPF problem effectively. Thus, a hybrid solver of PSO and SOCP is proposed in this study. Specifically, for the DES sizing with discrete energy capacity variables, PSO, as one of the advanced heuristic search methods, is more applicable, has a faster convergence speed, and has fewer algorithm parameters. For the DES scheduling with continuous charging/discharging power variables, among mathematical planning algorithms, SOCP has higher computational efficiency compared to other algorithms under the premise that the relaxation accuracy is the same, so SOCP is usually the first choice of relaxation techniques. With the siting decided using the MSCLSI-based sequential strategy, the DES sizing is jointly handled using PSO, with the scheduling under multiple scenarios addressed using SOCP. The relationship between the two parts is shown in Figure 1.

(1) DES sizing:

Considering the first layer from the DES investor's point of view, the establishment of equipment to participate in the power system electric energy market transactions and the auxiliary services market transactions of the investment planning model, this model takes into account the costs of investment CI, costs of degradation CD and savings of load shifting SLS. The objective function of this layer OF_1 is calculated as follows:

$$MinOF_1 = CI + CD - SLS \tag{19}$$

with the constraints of Equations (15)–(18) kept. Although the solution above is easy, the feasibility of solutions should also consider the constraints of DES scheduling. Thus, the solution of DES sizing needs to be set and optimized together with the objective function in DES scheduling.

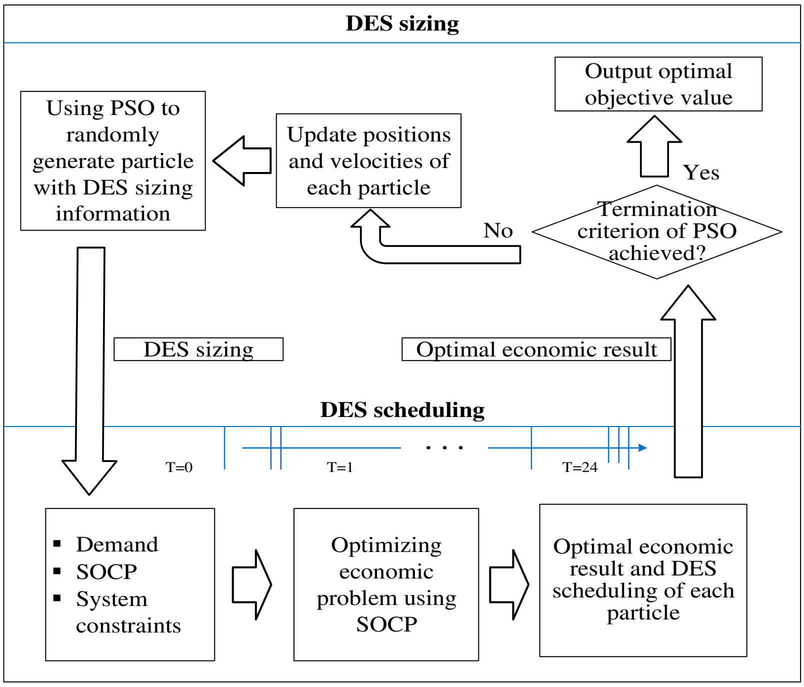

Figure 1. The relationship between DES sizing and scheduling.

(2) DES scheduling.

The second layer considers the operating cost of the grid-side DES configuration as well as the scheduling economics from the perspective of system operation economics. Therefore, the economic factors considered include costs of investment CI, cost of maintenance CM, cost of degradation CD, savings of load shifting SLS and savings of loss reduction SLR. The initialized or updated objective function OF_1 of the DES sizing is taken as known and optimized together with the savings as given in Equation (19).

$$Min\ OF_2 = CM + CI + CD - SLS - SLR \tag{20}$$

For simplicity, the subscript s is neglected in the following content of this section, to detail the cost–benefit analysis of a certain scenario. The constraints of the DES scheduling optimization above are represented by Equations (9)–(18).

3.2. DES Sizing Optimization Using PSO

Heuristic search methods can solve MINLP problems with global optimality through exhausted searches throughout the solution space. In this study, PSO is employed to address the inter-layer sizing optimization problem. Since its introduction in 1995, PSO has been extensively applied to solve different optimization problems in power systems [25].

3.3. DES Scheduling Optimization Using SOCP

The DES scheduling optimization is nonconvex and hard to solve directly due to the power flow constraints of Equations (9)–(11). In this study, a relaxation technique is used to convexify the original MINLP problem into solvable SOCP. Specifically, variables are redefined below for relaxation.

$$v_i^p = \left(V_i^P\right)^2 \tag{21}$$

$$L_{ij}^{p} = \frac{\left(P_{ij}^{p}\right)^{2} + \left(Q_{ij}^{p}\right)^{2}}{\left(V_{i}^{P}\right)^{2}} \tag{22}$$

v_i^p denotes the square of voltage magnitude at phase p of bus i; L_{ij}^p represents the square of branch current at phase p between buses i and j.

Combine Equations (21) and (22) into Equations (9)–(11),

$$P_{DG,i}^{p} + P_{ij}^{p} - \sum P_{jk}^{p} = -P_{j}^{p} + r_{ij}^{p} L_{ij}^{p} \tag{23}$$

$$Q_{DG,i}^{p} + Q_{ij}^{p} - \sum Q_{jk}^{p} = -Q_{j}^{p} + x_{ij}^{p} L_{ij}^{p} \tag{24}$$

$$v_{i}^{p} - v_{j}^{p} = 2\left(r_{ij}^{p} P_{ij}^{p} + x_{ij}^{p} Q_{ij}^{p}\right) - \left(\left(r_{ij}^{p}\right)^{2} + \left(x_{ij}^{p}\right)^{2}\right) L_{ij}^{p} \tag{25}$$

$$L_{ij}^{p} = \frac{\left(P_{ij}^{p}\right)^{2} + \left(Q_{ij}^{p}\right)^{2}}{v_{i}^{p}} \tag{26}$$

In (23), all the equations are linearized except for (26) with square items. To handle it, SOCP is adopted for relaxation as follows [26].

$$L_{ij}^{p} \geq \frac{\left(P_{ij}^{p}\right)^{2} + \left(Q_{ij}^{p}\right)^{2}}{v_{i}^{p}} \tag{27}$$

Equation (27) is then equivalent to Equation (28):

$$\left(P_{ij}^{p}\right)^{2} + \left(Q_{ij}^{p}\right)^{2} + \left(\frac{v_{i}^{p} - L_{ij}^{p}}{2}\right)^{2} \leq \left(\frac{v_{i}^{p} + L_{ij}^{p}}{2}\right)^{2} L_{ij}^{p} \geq \frac{\left(P_{ij}^{p}\right)^{2} + \left(Q_{ij}^{p}\right)^{2}}{v_{i}^{p}} \tag{28}$$

Equation (28) can be rewritten as Equation (29):

$$\left\| \begin{matrix} 2P_{ij}^{p} \\ 2Q_{ij}^{p} \\ v_{i}^{p} - L_{ij}^{p} \end{matrix} \right\|_{2} \leq v_{i}^{p} + L_{ij}^{p} \tag{29}$$

As SOCP is used to relax the original nonconvex problem, the accuracy of the solution after relaxation should be judged. Thus, a difference gap D is defined to calculate the error between the relaxed and the original power flow.

$$D = \left(P_{ij}^{p}\right)^{2} + \left(Q_{ij}^{p}\right)^{2} - v_{i}^{p} L_{ij}^{p} \tag{30}$$

The SOCP DES scheduling problem will be effectively solved using MATLAB2016a with CPLEX12.10 solvers.

4. MSCLSI-Based Sequential Placement Strategy

To account for the effects of DES charging and discharging under multiple operation scenarios, a multi-scenario comprehensive loss sensitivity index (MSCLSI) is specified and formulated as

$$CLSI_{s}^{r} = \lambda_{d} LSI_{d,s}^{r} - \lambda_{c} LSI_{c,s}^{r} \tag{31}$$

where $LSI_{d,s}^{r}$ and $LSI_{c,s}^{r}$ are the loss sensitivities corresponding to the discharging and charging of the r^{th} DES placement in scenarios, respectively, as given by

$$LSI_{c,s}^{r} = \frac{\partial P_{Loss,c,s}^{r}}{\partial P_{B,c,s}^{r}} = \left| \frac{P_{Loss,c,s}^{r} - P_{Loss,c,s}^{r-1}}{P_{c,s}^{r} - P_{c,s}^{r-1}} \right| \tag{32}$$

$$LSI_{d,s}^{r} = \frac{\partial P_{Loss,d,s}^{r}}{\partial P_{B,d,s}^{r}} = \left| \frac{P_{Loss,d,s}^{r} - P_{Loss,d,s}^{r-1}}{P_{d,s}^{r} - P_{d,s}^{r-1}} \right| \tag{33}$$

where λ_d and λ_c are the weights of discharging and charging loss sensitivities and can be adjusted in practice based on their durations and electricity prices so that $\lambda_d + \lambda_c = 1$. $P_{c,s}^{r}$ and $P_{d,s}^{r}$ represent the charging/discharging power at lowest/highest net load after r^{th} DES placement under scenario s.

To make the DES location selected using $MSCLSI_s^r$ more adaptable to multiple typical scenarios, the $MSCLSI_s^r$ for all scenarios are averaged as the final MSCLSI, with the calculation formula as follows:

$$MSCLSI^r = \sum\nolimits_{s=1}^{S} CLSI_s^r / S \tag{34}$$

The MSCLSI defined above considers the impacts of DES charging and discharging under multiple operation scenarios.

Based on the MSCLSI, a sequential placement strategy is then presented to support the applications of the proposed hybrid optimal DES placement in distribution networks. The complete process of the MSCLSI-based sequential placement strategy is detailed in Figure 2.

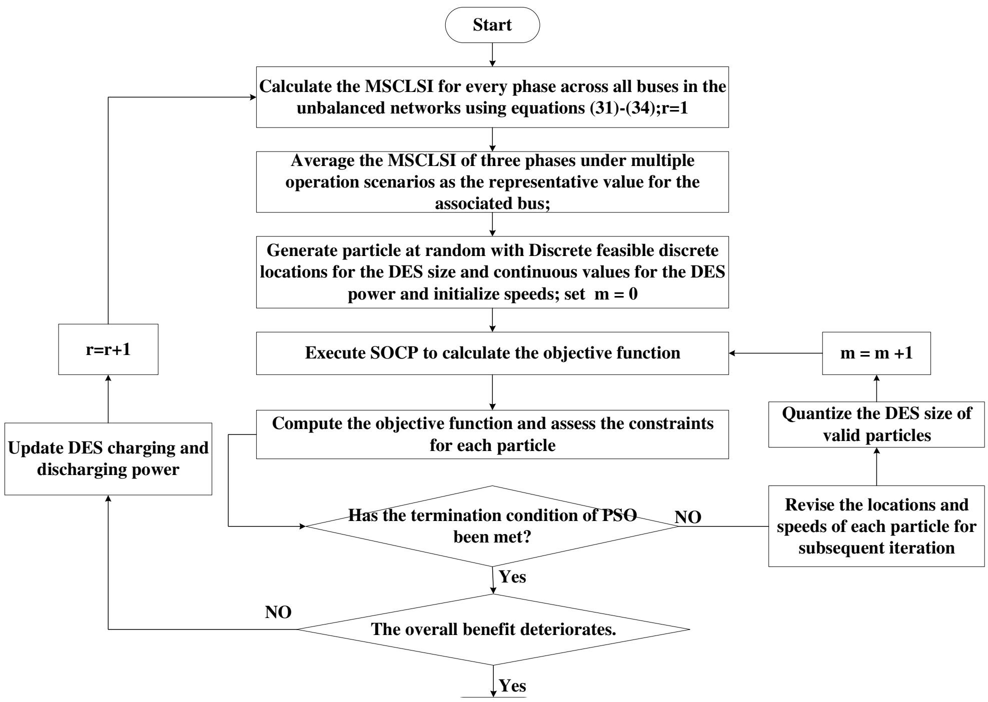

Figure 2. Flowchart of DES Sequential Placement based on MSCLSI.

5. Case Study

5.1. Simulated Network and Parameters Setting

To test the proposed hybrid optimization-based sequential DES placement model, the IEEE 33 node distribution system is taken as an example to simulate the analysis. As shown in Figure 3, a P_{pv1} = 400 kW and P_{pv2} = 700 kW PV power station is connected to nodes 7 and 30, respectively, where the loads are large, and one year's historical data from the two PV plants are used for analysis over each individual method [27]. DESs are assumed to be lithium-ion battery banks with superior life cycles and higher charge/discharge rates.

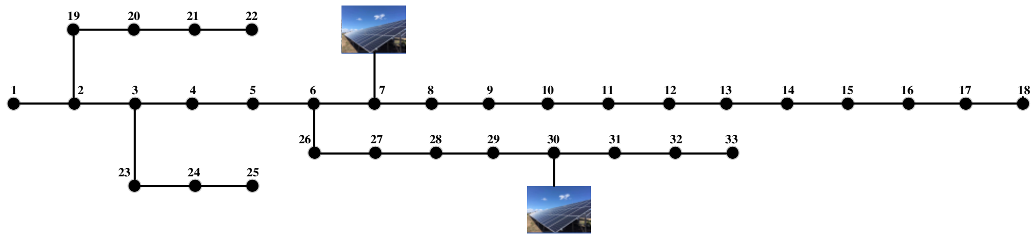

Figure 3. Simulated distribution network of IEEE 33 node.

5.2. DES Siting, Sizing and Scheduling

The proposed DES placement problem is solved for the unbalanced distribution network, with the placement results given in Table 1 and Figure 4. Specifically, bus 31 is first located with the highest MSCLSI for the 1st placement. Then, the optimal sizing and scheduling of DES is performed for bus 31. The quantities of DES units in phases A, B and C are 100, 100 and 100, respectively, marking a total DES capacity of 300 kWh. The objective function OF is \$−33,649.4, including the costs of investment CI \$5564.5, maintenance CM \$4989.3 and costs of degradation CD \$5342.1, as well as the savings of load shifting SLS \$44,664.2 and savings of loss reduction SLR \$4881.1, respectively.

Table 1. DES placement results of the proposed sequential strategy.

Placement	1st	2nd	3rd	4th	5th
Selected Bus	**31**	**5**	**7**	**30**	**4**
OF (\$)	−33,649.4	−41,630	−44,201.7	−47,034.9	−47,034.9
CM (\$)	4989.3	7786.8	9040.2	10,941.6	10,941.6
CI (\$)	5564.5	13,376.7	22,893	27,038.8	27,038.8
CD (\$)	5342.1	4435.7	3648.6	2854.8	2854.8
SLS (\$)	44,664.2	61,753.7	76,845.3	84,696.7	84,696.7
SLR (\$)	4881.1	5475.5	2938.2	3173.4	3173.4
BN (A/B/C)	100/100/100	100/108/100	107/108/110	110/110/110	0
E (kWh)	300	308	325	330	0

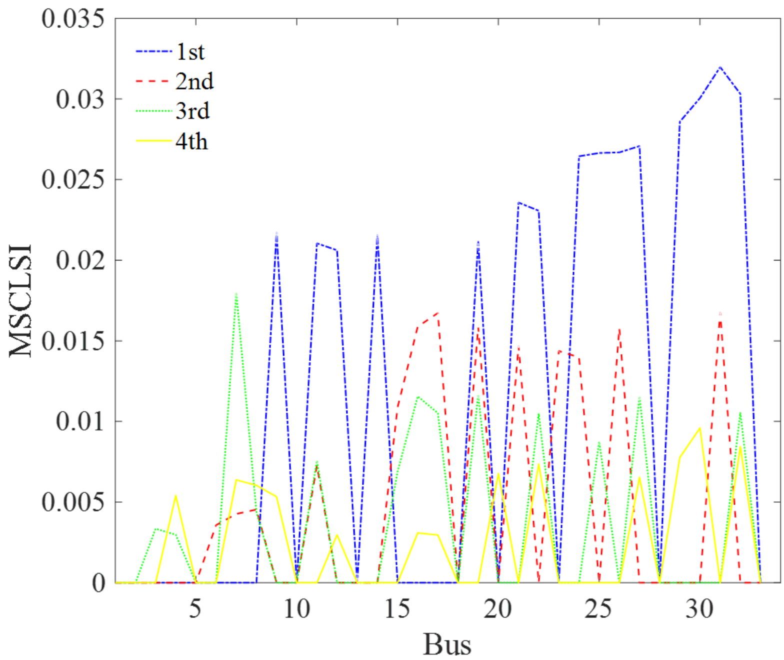

Figure 4. MCLSI profiles after the proposed sequential DES placements.

Taking the bus 31 placement as known, DES placement is continued based on the proposed sequential strategy. As shown in Table 1, buses 5, 7 and 30 are subsequently chosen for the 2nd, 3rd and 4th DES placements, with the objective function *OF* continuously reduced to \$−41,630, \$−44,201.7 and \$−47,034.9, respectively, which marks an increasing net profit. Correspondingly, the DES capacities of these three placements are 308 kWh, 325 kWh and 330 kWh. The objective function (*OF*) and individual objectives after the 5th placement stay the same as those after the 4th placement, with the DES capacity being zero. This indicates that the 5th placement would lead to a decrease in net profit due to costs surpassing the savings, making it financially unviable. Therefore, the result following the 4th placement is the most optimal for the simulated network. It is worth noting that as DES investment costs and capacity increase, there is a significant growth in the revenues from peaking ancillary services. This is because the returns in the peaking service market are largely dependent on the capacity of the energy storage device being built. It should also be noted that the savings of loss reduction continuously reduced from \$4881.1 for the 1st placement to \$5475.5, \$2938.2 and \$3173.4 for the remaining three placements. This is because DES is generally not designed for loss reduction but for peak shaving and valley filling. It can also be seen through Table 1 that as the number of placements increases, the DES degradation cost decreases from \$5342.1 to \$2854.8. DES charging/discharging is accompanied by chemical reactions and physical changes within the batteries, leading to capacity degradation and increased internal resistance, which in turn accelerates the DES lifetime loss. In this paper, the DES is sequentially placed, and the placement order determines the frequency and depth of DES charging and discharging as well as the balance of load distribution. Among the four placements, the DES assigned to node 31 takes a larger load and undergoes deeper and more frequent charging/discharging cycles than those assigned to nodes 5, 7 and 30, and therefore the DES assigned to node 31 is more validated for the costs of degradation than the other DESs. The daily net load profiles of four seasonal scenarios with and without DES are compared in Figure 5 below. It can be seen that DES has played a significant role in load shifting.

5.3. Performance Test of the Proposed Hybrid PSO-SOCP

Another main aspect of this study is suggesting the hybrid solution strategy of PSO-SOCP to balance optimization costs and accuracy. For comparison, the OPF problem of DES placement is solved again using PSO and SOCP, respectively, with the results given in Table 2. Considering PSO has the theoretical capability of global optimality by searching throughout the whole solution space, it is taken as the accuracy benchmark. The computation performance is marked using error for accuracy, which is calculated with Equation (25), and using time for efficiency. Specifically, in terms of accuracy, we conducted three sets of experiments, which were as follows: (1) SOCP processed the optimal placement of DES in a single scenario (E1); (2) PSO-SOCP processed the optimal placement of DES in a single scenario (E2); (3) PSO-SOCP processed the optimal placement of DES in multiple scenarios (E3). Then, we compared the difference gap between the three experiments in the same scenario and the result is shown in Figure 6. It can be seen that the difference gap of E2 is much smaller than E1. This is because relaxations and assumptions are made in SOCP, while PSO in the hybrid method has global optimality. Influenced by multiple operational scenarios, the difference gap of E3 is larger than E2 but smaller than E1. Although the accuracy of E3 is affected by the consideration of multiple scenarios, the benefit of placement is greatly improved. In terms of efficiency, we compared the solution time of PSO, SOCP and PSO-SOCP to optimize the single scenario DES placement problem. PSO as an independent method suffers a serious computation burden, making it the worst among the three methods. Compared to PSO, the proposed hybrid optimization is much faster and cost-acceptable. Therefore, the proposed PSO-SOCP hybrid optimization improves efficiency with guaranteed accuracy, which makes it more suitable for the proposed DES placement in unbalanced distribution networks under multiple operation scenarios.

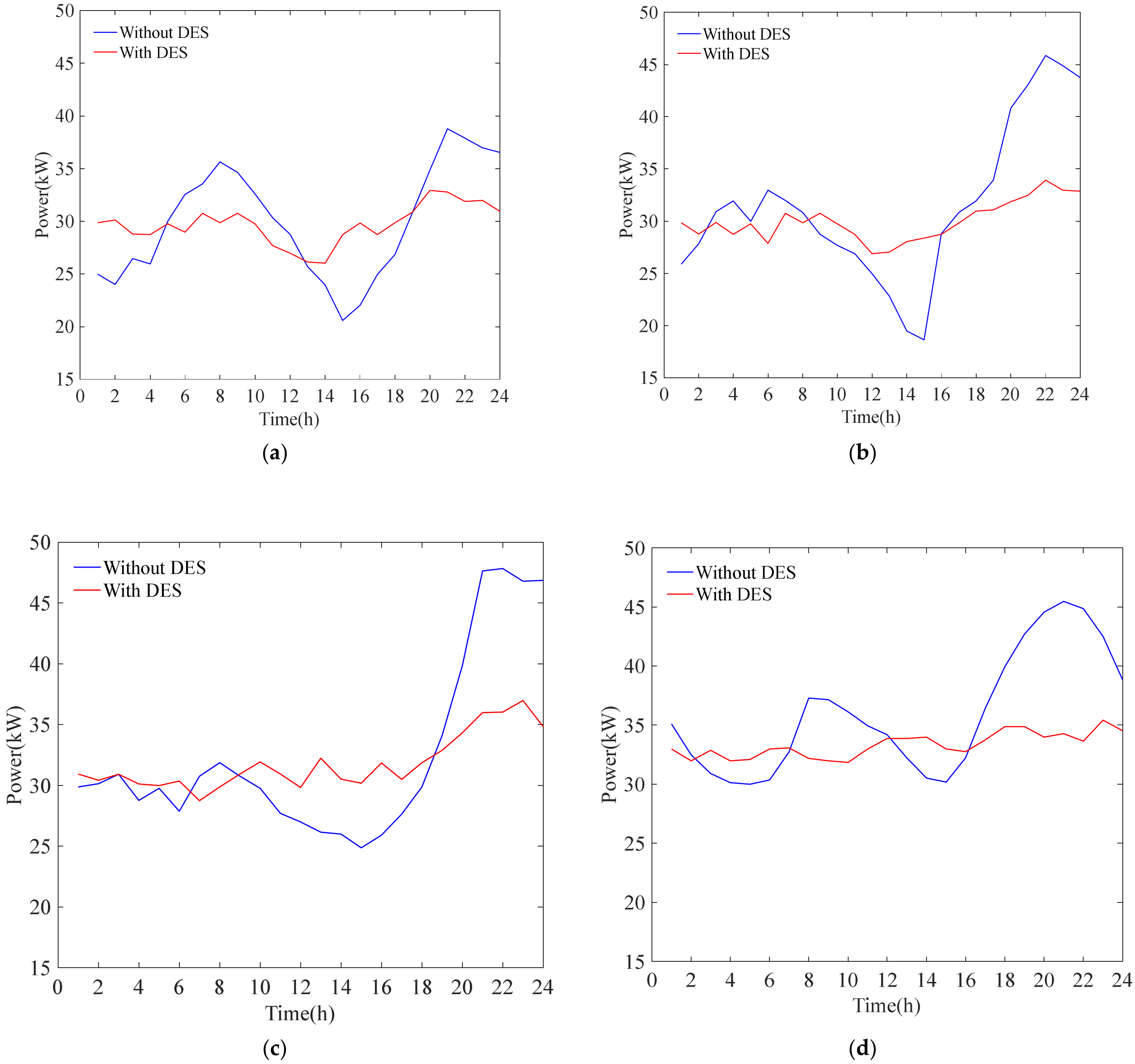

Figure 5. Daily net load profiles for MSCLSI-based simulated networks with and without DES: (**a**) spring, (**b**) summer, (**c**) autumn, (**d**) winter.

Table 2. Performance comparison of single and hybrid optimizations.

Algorithm	PSO	SOCP	PSO-SOCP
Time	22 h	142.34 s	156.44 s

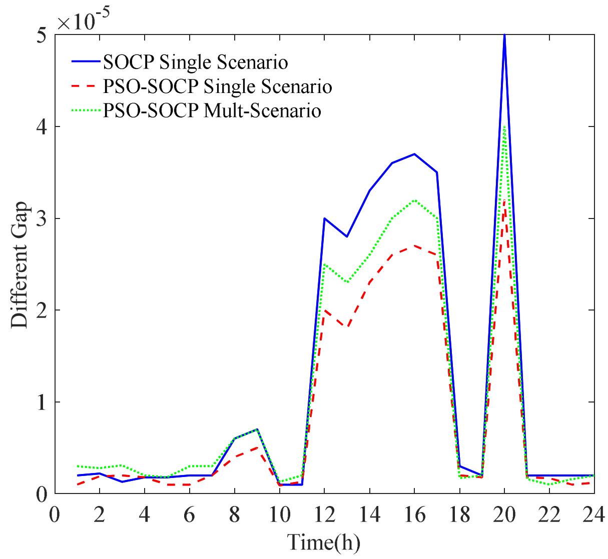

Figure 6. Hourly difference gap of distribution network under three cases.

5.4. Performance Test of the Proposed MSCLSI

Another key aspect of this study is suggesting the MSCLSI to take into account the effects of DES charging/discharging under multiple operation scenarios. To show its superiority, the proposed MSCLSI is compared against the single-scenario CLSI of spring, with the results given in Table 3. It can be observed that the four locations with the highest sensitivities are buses 31, 6, 9 and 30, which differ significantly from those (buses 31, 5, 7 and 30) identified using the proposed MSCLSI in Table 1. In detail, the savings of load shifting SLS using the proposed MSCLSI of \$44,664.2 are much higher than those of the single-scenario-based CLSI of \$37,842.3. Meanwhile, the DES considering the MSCLSI sequential placement has an expected gain of \$33,649.4, while the DES based on the CLSI placement has an expected gain of only \$25,724.5, which is 23.55% lower in comparison. This is because only the spring net load profile was considered when performing the MSCLSI, and the load and PV profiles of the four seasons vary significantly. Comparing Figures 5 and 7, it can be seen that the effect of the peak shaving and valley filling of other scenarios in the CLSI is not as strong as in the proposed MSCLSI. This is because the load and PV profiles of the four seasons vary significantly. Therefore, the proposed MSCLSI is more suitable for all scenarios, with the sensitivities of four typical scenarios averaged to decide the DES placement locations.

Table 3. DES placement results of the CLSI based sequential strategy.

Placement	**1st**	**2nd**	**3rd**	**4th**
Selected Bus	**31**	**6**	**9**	**30**
OF (\$)	−25,724.5	−28,013.8	−35,894.4	−39,231
CM (\$)	4989.3	6597.8	8967.5	9758.8
CI (\$)	5564.5	12,874.7	22,594	26,869
CD (\$)	4547.2	3843.3	2965.8	2674.8
SLS (\$)	37,842.3	46,652.8	67,954.8	75,985.8
SLR (\$)	2983.2	4676.8	2466.9	2547.8
BN (A/B/C)	100/100/100	90/100/90	107/108/110	100/100/100
E (kWh)	300	280	325	300

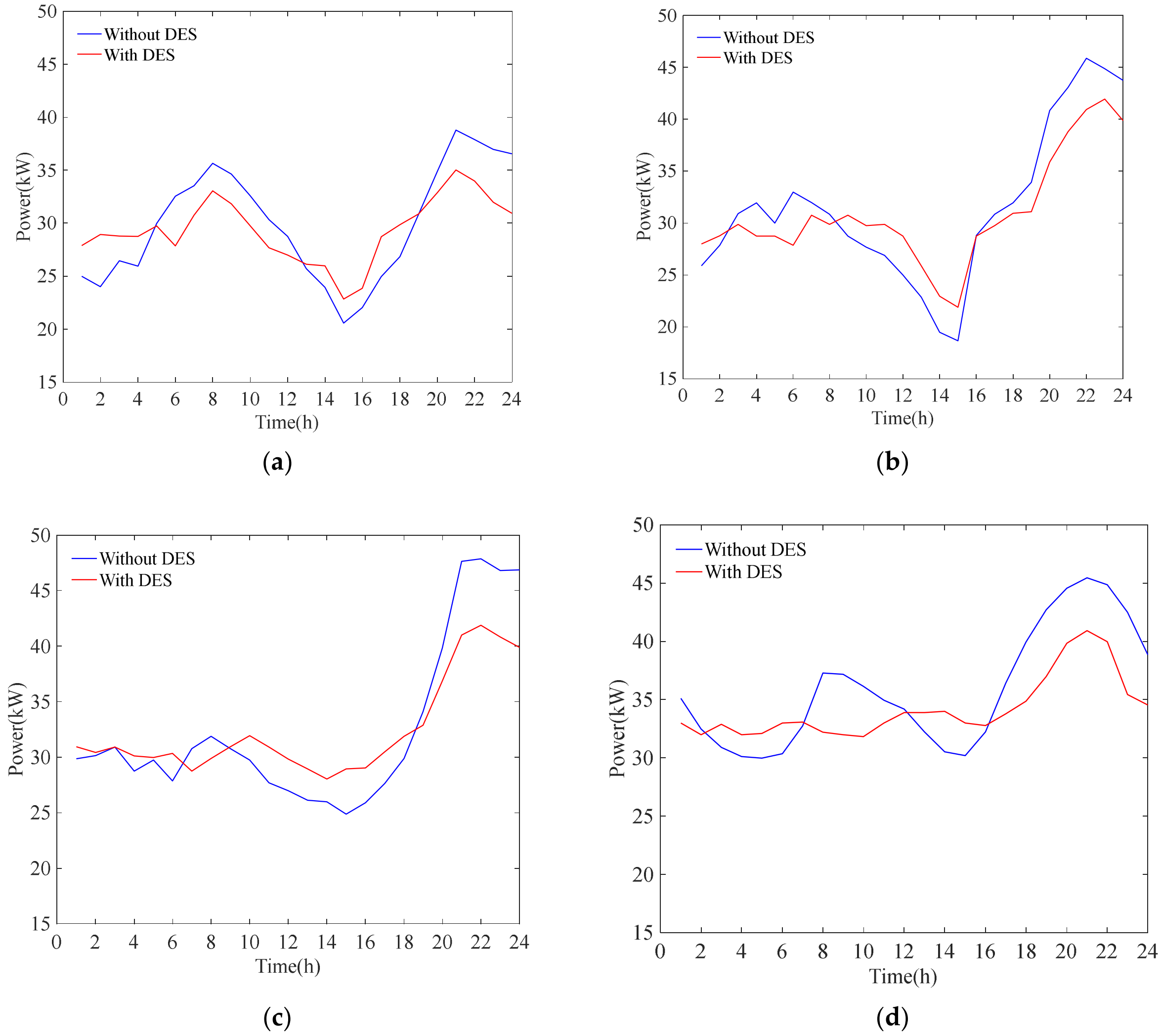

Figure 7. Daily net load profiles for CLSI-based simulated networks with and without DES: (**a**) spring, (**b**) summer, (**c**) autumn, (**d**) winter.

6. Conclusions

In this study, a sequential placement strategy is proposed, to determine the placement of DESs in unbalanced distribution networks. To solve the integrated DES sizing and scheduling problem, a hybrid solver of PSO-SOCP is proposed. The proposed hierarchical and sequential placement of DESs is tested by performing detailed simulations on the IEEE 33 distribution network. It can be concluded that: (i) the results of DES placement based on the MSCLSI are 36.47% lower in terms of expected gain compared to the results based on the CLSI, which indicates that the MSCLSI can better account for the impact of DES charging and discharging in multiple scenarios, and the results of the configuration are more reasonable; (ii) DES placement based on IEEE 33 shows that DES plays an important role in load shifting, and the proposed hierarchical and sequential strategy effectively takes into account the impact of the three-phase imbalance in the active distribution network, and the results are more consistent with the actual operation of the grid and more feasible; (iii) comparing the DES placement results produced with PSO, SOCP and the proposed PSO-SOCP, respectively, the hybrid solver of PSO-SOCP proposed in this paper achieves a better balance between efficiency and accuracy, making it more suitable for DES placement in large-scale networks and under various operation scenarios.

This paper focuses on the optimal allocation of DES in unbalanced networks in multiple scenarios. Based on the environment of multi-system development, considering the characteristics of DES with a small capacity, flexible layout and dispersion, the market mechanism suitable for DES participation can be specified in the future, and the way in which DES can coordinate with other adjustable flexible resources can be expanded.

Author Contributions: Conceptualization, X.S.; Methodology, R.S.; Software, X.Y.; Validation, P.Z.; Formal analysis, W.L.; Investigation, M.W.; Resources, F.L.; Supervision, J.Y. All authors have read and agreed to the published version of the manuscript.

Funding: This research received no external funding.

Data Availability Statement: The data presented in this study are available on request from the corresponding author (X.S.).

Conflicts of Interest: The authors declare no conflict of interest.

References

1. Liu, B.; Meng, K.; Dong, Z.Y.; Wong, P.K.C.; Ting, T. Unbalance Mitigation via Phase-Switching Device and Static Var Compensator in Low-Voltage Distribution Network. *IEEE Trans. Power Syst.* **2020**, *35*, 4865–4869. [CrossRef]
2. Gangwar, T.; Padhy, N.P.; Jena, P. Energy Management Approach to Battery Energy Storage in Unbalanced Distribution Networks. *IEEE Trans. Ind. Appl.* **2024**, *60*, 1345–1356. [CrossRef]
3. Ren, L.; Liao, W.; Chen, J. Systematic Design and Implementation Method of Battery-Energy Comprehensive Management Platform in Charging and Swapping Scenarios. *Energies* **2024**, *17*, 1237. [CrossRef]
4. De Oliveira, J.F.L.; de Mattos Neto, P.S.G.; Siqueira, H.V.; Santos, D.S.d.O., Jr.; Lima, A.R.; Madeiro, F.; Dantas, D.A.P.; Cavalcanti, M.d.M.; Pereira, A.C.; Marinho, M.H.N. Forecasting Methods for Photovoltaic Energy in the Scenario of Battery Energy Storage Systems: A Comprehensive Review. *Energies* **2023**, *16*, 6638. [CrossRef]
5. Zheng, Y.; Song, A.; Huang, A.; Hill, D.J. Hierarchical Optimal Allocation of Battery Energy Storage Systems for Multiple Services in Distribution Systems. *IEEE Trans. Sustain. Energy* **2020**, *11*, 1911–1921. [CrossRef]
6. Zhang, X.; Son, Y.; Choi, S. Optimal Scheduling of Battery Energy Storage Systems and Demand Response for Distribution Systems with High Penetration of Renewable Energy Sources. *Energies* **2022**, *15*, 2212. [CrossRef]
7. Tang, Y.; Low, S.H. Optimal Placement of Energy Storage in Distribution Networks. *IEEE Trans. Smart Grid* **2017**, *8*, 3094–3103. [CrossRef]
8. Wang, H.; Yan, Z.; Shahidehpour, M.; Zhou, Q.; Xu, X. Optimal Energy Storage Allocation for Mitigating the Unbalance in Active Distribution Network via Uncertainty Quantification. *IEEE Trans. Sustain. Energy* **2021**, *12*, 303–313. [CrossRef]
9. Pompern, N.; Premrudeepreechacharn, S.; Siritaratiwat, A.; Khunkitti, S. Optimal Placement and Capacity of Battery Energy Storage System in Distribution Networks Integrated with PV and EVs Using Metaheuristic Algorithms. *IEEE Access* **2023**, *11*, 68379–68394. [CrossRef]
10. Zhang, Y.X.; Ren, S.Y.; Dong, Z.Y.; Xu, Y.; Meng, K.; Zheng, Y. Optimal placement of battery energy storage in distribution networks considering conservation voltage reduction and stochastic load composition. *IET Gener. Transm. Distrib.* **2017**, *11*, 3862–3870. [CrossRef]
11. Wong, L.A.; Ramachandaramurthy, V.K.; Walker, S.L.; Ekanayake, J.B. Optimal Placement and Sizing of Battery Energy Storage System Considering the Duck Curve Phenomenon. *IEEE Access* **2020**, *8*, 197236–197248. [CrossRef]
12. Thrampoulidis, C.; Bose, S.; Hassibi, B. Optimal Placement of Distributed Energy Storage in Power Networks. *IEEE Trans. Autom. Control* **2016**, *61*, 416–429. [CrossRef]
13. Wichitkrailat, K.; Premrudeepreechacharn, S.; Siritaratiwat, A.; Khunkitti, S. Optimal Sizing and Locations of Multiple DESs in Distribution Systems Using Crayfish Optimization Algorithm. *IEEE Access* **2024**, *12*, 94733–94752. [CrossRef]
14. Giannitrapani, A.; Paoletti, S.; Vicino, A.; Zarrilli, D. Optimal Allocation of Energy Storage Systems for Voltage Control in LV Distribution Networks. *IEEE Trans. Smart Grid* **2017**, *8*, 2859–2870. [CrossRef]
15. Alsharif, H.; Jalili, M.; Hasan, K.N. A Frequency Stability Analysis for DES Placement Considering the Loads and Wind farms Locations. In Proceedings of the 2022 IEEE PES 14th Asia-Pacific Power and Energy Engineering Conference (APPEEC), Melbourne, Australia, 20–23 November 2022.
16. Das, C.K.; Bass, O.; Kothapalli, G.; Mahmoud, T.S.; Habibi, D. Overview of energy storage systems in distribution networks: Placement, sizing, operation, and power quality. *Renew. Sustain. Energy Rev.* **2018**, *91*, 1205–1230. [CrossRef]

17. Su, X.; Zhang, Z.; Liu, Y.; Fu, Y.; Shahnia, F.; Zhang, C.; Dong, Z.Y. Sequential and Comprehensive BESSs Placement in Unbalanced Active Distribution Networks Considering the Impacts of BESS Dual Attributes on Sensitivity. *IEEE Trans. Power Syst.* **2021**, *36*, 3453–3464. [CrossRef]
18. Kersting, W.H. Distribution line models. In *Distribution System Modeling and Analysis*, 3rd ed.; CRC: Boca Raton, FL, USA, 2012; Volume 9, pp. 313–342.
19. Ma, J.; Venkatesh, B. Sizing Merchant Energy Storage for Maximum Revenues Considering Net Metering and Ancillary Services. *IEEE Access* **2024**, *12*, 2210–2223. [CrossRef]
20. Zhou, P.; Chen, Q.; Xia, Q.; He, G.; Kang, C. Evaluating the Contribution of Energy Storages to Support Large-Scale Renewable Generation in Joint Energy and Ancillary Service Markets. *IEEE Trans.* **2016**, *7*, 808–818.
21. Calero, F. A Review of Modeling and Applications of Energy Storage Systems in Power Grids. *Proc. IEEE* **2023**, *7*, 806–831. [CrossRef]
22. Frank, S.; Steponavice, I.; Rebennack, S. Optimal power flow: A bibliographic survey II. *Energy Syst.* **2012**, *3*, 259–289. [CrossRef]
23. Li, X.; Wang, L.; Yan, N.; Ma, R. Cooperative Dispatch of Distributed Energy Storage in Distribution Network with PV Generation Systems. *IEEE Trans. Appl. Supercond.* **2021**, *31*, 0604304. [CrossRef]
24. Kennedy, J.; Eberhart, R. Particle swarm optimization. In Proceedings of the ICNN'95—International Conference on Neural Networks, Perth, Australia, 27 November–1 December 1995; Volume 4, pp. 1942–1948.
25. Yu, P.; Wan, C.; Song, Y.; Jiang, Y. Distributed Control of Multi-Energy Storage Systems for Voltage Regulation in Distribution Networks: A Back-and-Forth Communication Framework. *IEEE Trans. Smart Grid* **2021**, *12*, 1964–1977. [CrossRef]
26. Low, S.H. Convex Relaxation of Optimal Power Flow—Part I: Formulations and Equivalence. *IEEE Trans. Control Netw. Syst.* **2014**, *1*, 15–27. [CrossRef]
27. Baran, M.E.; Wu, F.F. Network Reconfiguration in Distribution Systems for Loss Reduction and Load Balancing. *IEEE Power Eng. Rev.* **1989**, *9*, 101–102. [CrossRef]